

1 **Influence of wood density in tree-ring based annual**
2 **productivity assessments and its errors in Norway**
3 **spruce.**

4

5

6 **O. Bouriaud¹, M. Teodosiu¹, A. V. Kirdyanov², C. Wirth^{3,4}**

7

8 [1] {Forest Research and Management Institute, Station Câmpulung Moldovenesc,
9 Calea Bucovinei 73b, 725100 Câmpulung Moldovenesc, Romania}

10 [2] {V.N. Sukachev Institute of Forest SB RAS, Akademgorodok, Krasnoyarsk,
11 660036 Russia}

12 [3] {Institute of Biology, University of Leipzig, Johannisallee 21-23, 04103 Leipzig,
13 Germany}

14 [4] {German Centre for Integrative Biodiversity Research (iDiv) Halle-Jena-Leipzig,
15 Deutscher Platz 5e, 04103 Leipzig, Germany}

16 Correspondence to: O. Bouriaud (obouriaud@gmail.com)

17

18 **Abstract**

19 Estimations of tree annual biomass increments are used by a variety of studies related
20 to forest productivity or carbon fluxes. Biomass increment estimations can be easily
21 obtained from diameter surveys or historical diameter reconstructions based on tree
22 rings records. However, the biomass models rely on the assumption of a constant
23 wood density. Converting volume increment into biomass also requires assumptions
24 on the wood density. Wood density has been largely reported to vary both in time and
25 between trees. In Norway spruce, wood density is known to increase with decreasing
26 ring width. This could lead to underestimating the biomass or carbon deposition in
27 bad years. The variations between trees of wood density has never been discussed but
28 could also contribute to deviations. A modelling approach could attenuate these
29 effects but will also generate errors.

30 Here were developed a model of wood density variations in Norway spruce, and an
31 allometric model of volume growth. We accounted for variations in wood density
32 both between years and between trees, based on specific measurements. We compared
33 the effects of neglecting each variation source on the estimations of annual biomass
34 increment. We also assessed the errors of the biomass increment predictions at tree
35 level, and of the annual productivity at plot level.

36 Our results showed a partial compensation of the decrease in ring width in bad years
37 by the increase in wood density. The underestimation of the biomass increment in
38 those years reached 15%. The errors related to the use of an allometric model of
39 volume growth were modest, around $\pm 15\%$. The errors related to variations in wood
40 density were much larger, the biggest component being the inter-tree variability. The
41 errors in plot-level annual biomass productivity reached up to 40%, with a full
42 account of all the error sources.

43

44 Key words: Forest biomass, Uncertainty propagation, Bayesian framework, Wood
45 density, Norway spruce, tree-ring

46

47 **1 Introduction**

48 Predicting trees biomass increment is a key step in quantifying and understanding
49 forest productivity. Considerable efforts have been spent to evaluate forest
50 productivity and carbon sink strength (Ciais et al., 2008). While productivity has long
51 referred to volume growth, amply used in the forest management and displayed in
52 yield tables, the focus recently switched to biomass, for its relationships with energy
53 or carbon storage. Field-based estimations of biomass growth have a wide variety of
54 applications, from forestry to carbon fluxes estimation, for example in comparison
55 against eddy covariance (Barford et al., 2001; Rocha et al., 2006; Gough et al., 2008;
56 Curtis et al., 2011; Ilvesniemi et al., 2011). Considerable efforts have been spent to
57 estimate annual forest productivity in relation to climate fluctuations and forests
58 carbon sink strength (Richardson et al., 2010; Wu et al., 2013). The importance of
59 having both annual resolution and high spatial coverage has been illustrated by
60 numerous studies (e.g. Reichstein et al., 2003; Ciais et al., 2005; Beer et al., 2010).
61 Several methods are used to estimate forest productivity and carbon sink: eddy
62 covariance, modelling, or field-based estimations such as inventories or tree-ring
63 studies. Tree-ring based studies have the advantage of offering a large spatial
64 covering, a potentially long time scale and also an annual resolution. They are
65 therefore amply used to produce reference annual biomass production estimations, to
66 compare against other methods (Beck et al., 2011; Babst et al., 2014a) or to bring
67 complementary information (Babst et al., 2013). However several issues are
68 associated to the use of tree-ring based estimations and the estimation of their error
69 remains a critical poorly documented (Nickless et al., 2011).

70 In the reconstruction of the annual productivity or of the above-ground carbon uptake
71 from field-based studies, one limiting element is the estimation of the wood density
72 variations (Babst et al., 2014a). Indeed, volume increment time series can be produced
73 by a variety of methods, such as the reconstruction of the diameter growth based on
74 tree rings (Wirth et al., 2004; Rocha et al., 2006) or inventory reconstruction (Ohtsuka
75 et al., 2007), but none of these methods bring information on the variation of wood
76 density. Converting volume into biomass requires an estimation of the wood density,
77 which is most likely based on literature and therefore neither related to site conditions,
78 nor to trees growth rate, as for example in Vila et al., (2013). In the same manner,
79 biomass equations implicitly rely on the use of an average and constant wood density

80 despite the many evidences of substantial wood density variations. In both cases,
81 wood density is considered constant in time, and equal between trees.

82 Wood density has however been acknowledged as a highly variable characteristic and
83 several major sources of annual density variations have been identified. Very high
84 precision in the description of the wood density variations with new techniques (e.g.
85 SilviScan, Evans, 1994) are possible but not widely available, while other techniques
86 based on X-ray are rather time consuming and thus not applied to forest productivity
87 studies. Within-tree variations occur at distinct time scales (Jyske et al., 2007). Over
88 medium or long scales, annual wood density was proved to be related to ring age or to
89 tree diameter, with higher values close to the pith in many species (Schweingruber,
90 1988). At inter-annual scale, wood density variations can be substantial. There were
91 several reports that (annual) ring density decreases with increasing ring width, for
92 instance in Norway spruce (Bergqvist, 1998; Dutilleul et al., 1998; Lundgren, 2004;
93 Bouriaud et al., 2005; Franceschini et al., 2010; 2013). Wood density was also proved
94 to vary between trees (Wilhelmsson et al., 2002; Guilley et al., 2004), a fact which is
95 never accounted for in studies using diameter surveys to produce biomass increment
96 estimations.

97 The variations of wood density between trees and between years could compensate
98 the variations in annual volume increment, or at least soften them. Recent studies
99 brought evidences of such compensation, proving that neglecting annual wood density
100 fluctuations could lead to substantial errors or bias in estimating the biomass (Molto
101 et al., 2013; Babst et al., 2014a). The errors generated by neglecting the variations in
102 wood density have been considered as small compared to those resulting from that of
103 the volume increment estimation, but to our knowledge, such assumptions were never
104 tested and the consequences not documented.

105 To be properly quantified, the consequences of neglecting wood density fluctuations
106 between years and between trees had to be tested using an integrated approach,
107 whereby the errors of the density model are propagated and combined with those of
108 the model for volume growth. Such chain can be decomposed, and the impact of each
109 step studied by modelling the steps into a single Monte Carlo Markov Chain (MCMC)
110 process (e.g. Molto et al., 2013). Analytical solutions to estimate the biomass
111 estimation error, based e.g. on Taylor expansion can sometimes be determined,
112 depending on the model's complexity. But the errors of biomass increment, obtained

114 by subtracting subsequent estimations, are anyhow less predictable and particularly
115 challenging at the plot level, when summing tree-level estimations (Nickless et al.,
116 2011). The MCMC approach therefore appears as the most suitable to estimate the
117 biomass increment, where such estimations and the propagation of the errors from one
118 model to another is done without assumptions.

119 Our study aimed at quantifying the impact of density variations, both between years
120 and between trees, on the estimations of annual biomass increment in Norway spruce
121 (*Picea abies*), and compare it with the impact of volume increment estimation errors.
122 The objectives were: (i) to quantify and model the influence of annual radial growth
123 variations on wood density, (ii) to quantify the consequences of annual and between
124 tree variations of wood density on biomass increment estimations and (iii) to compare
125 the errors related to wood density estimations to those of volume increment.

126

127

128 **2 Material and methods**

129

130 **2.1 Site, sampling and data**

131 All samples analysed for this study were taken from the Wetzstein site near the village
132 of Lehesten in Thuringia, Central Germany (50°45'N, 11°46'E, ~ 760 m a.s.l.), which
133 was amply used for eddy covariance measurements (e.g. Anthoni et al., 2004) or
134 biomass modeling (Wirth et al., 2004). The site is characterised by mono-specific
135 Norway spruce (*Picea abies* L.) stands. The climate is typical for the mid-elevation
136 montane sites with an annual mean temperature of 6°C and a mean annual
137 precipitation sum of ~1000 mm. Soils have a sandy loam texture. The footprint of the
138 eddy covariance tower is dominated by an extensive 80 (± 2.1 SD) year old stand. This
139 stand is mostly even-aged but also contains pockets of regeneration and scattered
140 emergent trees. The footprint stand is surrounded by three even-aged stands with a
141 mean age of 15 (± 0.86), 38 (± 7.9) and 116 (± 1.3) years. The four stands representing
142 the site are referred as W15, W38, W72 and W116

143 This study combines data from three successive samplings realized in this site: (i)
144 Stem analysis performed to quantify the relationship between breast-height radial

146 growth and stem volume increment. This was achieved in connection with a biomass
147 harvest of the four stands (see below). (ii) Wood density measurements were done for
148 selected harvest trees to establish a relation between ring-width and wood density
149 variations, and (iii) a dendro-chronological analysis of inter-annual growth variation
150 of many trees using micro-cores for scaling up to the plot-scale. The volume
151 increment and wood density and volume increment measurements are used
152 exclusively to develop models, while the micro-cores sampling is used as an
153 application to quantify and compare the errors of each model on this representative
154 case study.

155 2.1.1 Stem analysis for volume increment

156 The stem volume increment model was fit based on a stem analysis realized on 22
157 trees – seven samples in the footprint stand W72 and five in each of the additional
158 stands (W15, W33, W116). Trees were selected to represent seven/five dbh (diameter
159 at breast height) classes defined based on the population of all inventoried trees (W15:
160 n = 144, W38: n = 59, W72: n = 133, W116: n = 68). Jointly, the 22 trees represented
161 the size range (dbh between 7.3 and 59.5 cm) and age range (between 14 and 117
162 years) of Norway spruce trees at the Wetzstein site. This comprehensiveness ensures
163 applicability of the models for all trees in the inventories of the test site. Trees were
164 felled in the context of a full biomass harvest. The circumference was measured every
165 meter along the bole where a 3-8 cm thick disc was cut in order to determine annual
166 increment along the entire stem. All discs were dried and sanded with a belt grinder.
167 The ring width series was measured along four radii on each disc. The average
168 diameter increment measured on the lower and upper disc of each 1 to 2 m segment
169 was used to calculate the increment of under bark volume in successive years using
170 the formula for a truncated cone. The difference in volumes of all segments per tree of
171 successive annual time steps yielded stem dry wood production of individual trees.
172 The dendrochronological analysis was carried out using a digital tree ring
173 measurement device (LINTAB III Digital Linear Table; 410-1/100-HF-130, Frank
174 Rinn Distribution, Heidelberg, Germany) in combination with the software TSAP
175 (Time Series Analysis Program, Frank Rinn Distribution, Heidelberg, Germany).

176

177 2.1.2 Wood density measurements

178 For the annual wood density (WD) measurements wood discs were sampled at breast
179 height from trees representing the lowest, the central and the highest diameter class in
180 each of the four stands. This yielded a total of 12 sample trees, again representing the
181 size and age range of Norway spruce tree at the site. Two 1-2 cm-wide slices from
182 opposite radii were sawn from the wood discs, for which wood density was measured
183 by X-ray densitometry in the densitometric Laboratory of Krasnoyarsk, Russia
184 (Walesch Electronics, Switzerland) using the standard procedure described by
185 Schweingruber (1988). Longitudinal strips with a constant thickness of 1.2 mm were
186 sawn, air dried, and exposed to X-ray radiations for 1 h on a Kodak TL film using
187 standard exposure conditions: acceleration tension of 8.5 kV, flux intensity of 15.0
188 mA, distance to the source of 3.5 m. Annual wood density (WD, kg m^{-3}) values were
189 obtained from density profiles of single tree-rings as the total mass of earlywood and
190 latewood divided by tree-ring width. X-ray derived densities represent dry wood.
191 Rescaling to fresh wood dimensions was not done as all ring-width series (stem
192 analysis and micro-cores) were measured on dry wood.

193

194 2.1.3 Application dataset

195 The volume increment and WD models were applied together on an independent set
196 of trees sampled in 13 randomly placed inventory plots inside the footprint stand
197 W72. The plots were established within the context of the project FORCAST (Rey
198 and Jarvis, 2006). From 31 to 62 trees per plots (551 in total) with diameter varying
199 from 8 to 51 cm (thus well within the range of the sample trees) were sampled for
200 historical diameter reconstruction based on micro-cores. The micro-cores enabled the
201 reconstruction of the past growth over the last 10 years only, since these short cores
202 are ~2 cm long. The diameter was reconstructed based on the simple assumption of
203 proportionality of the bark thickness to the diameter using the external diameter of the
204 trees at sampling.

205 2.2 Wood density and annual volume increment modelling

206 Models of WD or annual volume increment were fit using both maximum likelihood
207 methods and MCMC approach. The structure of the two models was first determined

209 using likelihood fits before being implemented in a Bayesian MCMC framework
210 using WinBUGS 1.4 (Spiegelhalter et al., 2003), based on the same datasets exactly,
211 using non-informative flat priors. The maximum-likelihood estimations were realized
212 using the nlme package (version 3.1-102, Pinheiro et al., 2011) of R (R version 3.0.1,
213 R Development Team, 2014).

214

215 2.2.1 The wood density model

216 Following recent publications on Norway spruce wood density (Franceschini et al.,
217 2010; 2013), the diameter and the ring cambial age (as counted from the pith) were
218 used as independent variables. The selection of the model was based both on the AIC
219 (Akaike Information Criterion) and the examination of the residual distribution. Fixed
220 and random tree-level effects were considered. The principle of parsimony was also
221 followed in the model building process, and random effect parameters were
222 considered only if improvements were observed based on the likelihood ratio test.

223 Several candidate models were tested, as follows

$$224 \quad WD_{ij} = a_0 + a_1RW_{ij} + a_2RW_{ij}^2 + \frac{a_3}{X_{ij}} + \varepsilon_{ij} \quad (1)$$

$$225 \quad WD_{ij} = a_0 + \frac{a_1}{1 + RW_{ij}} + \frac{a_2}{X_{ij}^{a_3}} + \varepsilon_{ij} \quad (2)$$

$$226 \quad WD_{ij} = a_0 + a_1RW_{ij}^{a_2} + \frac{a_3}{X_{ij}^{a_4}} + \varepsilon_{ij} \quad (3)$$

227 where i denotes the tree and j the year, $a_0 \dots a_4$ are fixed effects and potentially random
228 tree-level effects, X is either DBH or cambial age, $\varepsilon \approx N(0, \sigma^2)$. Random effects are
229 assumed to be normally distributed.

230

231 2.2.2 The annual volume increment model

232 The annual volume increment was modelled as a non-linear function of ring width
233 and tree diameter, based on the annual estimations of volume growth resulting from
234 the detailed stem analysis. The model reflects the fact that, for a given ring width,
235 volume increment depends strongly on the current size of the tree, here its diameter,

Olivier Bouriaud 13/7/15 10:52

Deleted: several independent variables were tested, such as

238 mostly for geometrical reasons. The taper was therefore not supposed to be constant
239 in time, and the trends in tree growth with age were directly absorbed in the model
240 since the volume increments resulted directly from the stem analysis measurements,
241 not from using models. Another specificity of this model was the specification of a
242 variance function in order to cope with the heteroscedasticity in the errors. The
243 resulting model is given in equation 4 and includes random coefficients for the
244 exponent b_3 :

$$245 \quad \Delta Vol_{ij} = b_0 + b_1 DBH_{ij}^{b_2} RW_{ij}^{b_3} + \varepsilon_{ij} \quad (4)$$

246 where $b_{3,i} = c_3 + d_{3,i}$ is the sum of a fixed parameter c_3 and a random tree-level term
247 $d_{3,i} \sim N(0, \sigma_{d3})$ that varied for each tree i .

248 The residual ε_{ij} was modeled as a power function of the diameter:

$$249 \quad \varepsilon_{ij} = b_4 + DBH^{b_5} \quad (5)$$

250

251 **2.3 Application to a case study, scenarios of biomass increment**

252 The micro-cores dataset was used as a concrete case study for estimating the
253 consequences of wood density variations and comparing the errors resulting from the
254 wood density and from the volume increment model. Both models were fit based on
255 their specific datasets within the MCMC framework, then the parameters and the
256 variance terms estimated were applied to compute the biomass increment of the
257 micro-cores trees, which represents an external set. The models were therefore fit
258 using the same structure as that used in the likelihood method, the parameters
259 estimated being further used to produce estimations of WD or annual volume
260 increment on the micro-core trees. Having both the fitting and the application run in a
261 single MCMC loop enables the propagation of the errors of each model.

262 The tree-level biomass increment estimations were the product of the WD and the
263 volume increment, then summed up to obtain stand-level per-ha biomass estimations
264 based also on the plot size. But according to the way the errors could be accounted
265 for, four different scenarios were distinguished:

Olivier Bouriaud 8/7/15 15:29

Deleted: produce

267 1) The baseline scenario was using a constant wood density set to be equal to the
 268 average observed value across the dataset (475 kg m^{-3}). The volume increment is
 269 estimated based on the model fitted but without considering random tree-level
 270 variations (using the fixed part of the model only) and without residual error ($\varepsilon_{ij}=0$).

271 Thus, for tree i and year j , the biomass increment was computed as

$$272 \quad \Delta B_{ij} = 0.475 \cdot \Delta Vol_{ij} \quad \text{where } \Delta Vol_{ij} = b_0 + b_1 DBH_{ij}^{b_2} RW_{ij}^{b_3}$$

273 Only the fixed part of the parameters b_0 to b_3 was used.

274 2) In the second scenario, the annual wood density was held constant but the volume
 275 increment included both the random tree-level variation and the residual error.

276 For tree i and year j , the biomass increment was computed as:

$$277 \quad \Delta B_{ij} = 0.475 \cdot \Delta Vol_{ij} \quad \text{with } \Delta Vol_{ij} = b_0 + b_1 DBH_{ij}^{b_2} RW_{ij}^{b_{3,i}} + \varepsilon_{ij} \quad (6)$$

278 where $b_{3,i} = c_3 + d_{3,i}$ is the sum of a fixed parameter c_3 and a random tree-level term
 279 that varied for each tree i and sampled as: $d_{3,i} \sim N(0, \sigma_{d3})$, σ_{d3} being estimated from
 280 the volume increment fit dataset. Thus, the parameter d_3 for the application varies
 281 from tree to tree and is being sampled from within the variability observed in the fit
 282 set. ε (the residual variation) is computed as a function of the diameter as presented
 283 in Eq. 5. All the parameters and the variance estimations were made by the Bayesian
 284 model within the MCMC loop.

285 3) In the third scenario, the biomass increment was defined as the product of the
 286 parametric estimations of both the WD and the annual volume increment: here only
 287 the fixed part of the models was used to produce both the WD and the volume
 288 increment estimations, while not accounting for random effects or residual variance.
 289 This represents the most common and probable use of such models, when no data are
 290 available for a calibration.

$$291 \quad \Delta B_{ij} = WD_{ij} \cdot \Delta Vol_{ij} \quad \text{where}$$

$$292 \quad WD_{ij} = a_0 + a_1 RW_{ij}^{a_2} + \frac{a_2}{DBH_{ij}^{a_3}} \quad \text{and } \Delta Vol_{ij} = b_0 + b_1 DBH_{ij}^{b_2} RW_{ij}^{b_3}.$$

293 Only the fixed part of the parameters are used.

294 4) In the last scenario, a full error propagation was conducted: the random and the
295 residual errors of both the WD and the volume increment models were used to
296 produce the biomass increment estimation.

$$297 \quad \Delta B_{ij} = WD_{ij} \cdot \Delta Vol_{ij} \quad \text{with } WD_{ij} = a_{0,i} + a_{1,i} RW_{ij}^{a_2} + \frac{a_{3,i}}{DBH_{ij}^{a_4}} + \varepsilon_{ij}$$

298 having $\forall k \in (0,1,3)$, $a_{k,i} = \alpha_k + a_{k,i}$ where α_k is the fixed part of the parameter, a_k
299 the random component, $a_{k,i} \sim N(0, \sigma_{ak})$ and $\varepsilon_{ij} \sim N(0, \sigma_{WD})$ where σ_{WD} is the residual
300 variance, estimated on the WD fit set.

301 $\Delta Vol_{ij} = b_0 + b_1 DBH_{ij}^{b_2} RW_{ij}^{b_{3,i}} + \varepsilon_{ij}$ with $b_{3,i} = c_3 + d_{3,i}$ and $d_{3,i} \sim N(0, \sigma_{d3})$ as in scenario
302 2, and $\varepsilon_{ij} \sim N(0, \sigma_{\Delta Vol})$ where $\sigma_{\Delta Vol}$ is the residual variance, estimated on the
303 volume increment fit set.

304 Thus, four different biomass increment estimations were produced, according to the
305 density estimation and the error propagation, and their difference summed at plot
306 level. In all the scenarios, volume increment was estimated based on measured ring
307 width series and the historical diameter of the trees.

308 The MCMC process generated posterior distributions of the model parameter
309 estimates, with their associated errors, and the estimations of the variance of the
310 random effects based on the Metropolis-Hastings algorithm over 10^4 iterations. It also
311 produced estimations of wood density, a volume increment computed from the fitted
312 model and applied to new data, along with a prediction uncertainty interval, here
313 represented by the range between 2.5 and 97.5% of the estimates distribution density.
314 The first 4000 iterations were used as pre-convergence and thus were excluded from
315 estimations, which were based on subsequent iterations only.

316

317 **3 Results**

318

319 **3.1 Describing wood density variability**

320 The (annual) ring wood density (WD) varied from 287 to 787 kg m⁻³ with within-trees
321 variations as considerable as variations between trees. Individual tree-ring series
322 showed a reduced WD in the first 5-10 years, followed by a linear increase up to 60
323 years and then fluctuated around a tree-specific sill (Fig. 1a). Variations difference
324 between two successive years reached 200 kg m⁻³.

325

326 Figure 1.

327

328 Variations in WD were mostly related to ring width with a linear correlation of -0.75
329 ($t = -39.23$, $df = 1199$, $p\text{-value} < 10^{-4}$) when pooling the data from all cores (Fig. 1b).
330 As shown in figure 1, WD series with very distinct average density values were
331 seemingly following the same linear pattern. The correlation with age was not as high
332 ($R_{\text{Pearson}} = 0.38$, $t = 14.25$, $df = 1199$, $p\text{-value} < 10^{-4}$).

333

334 **3.2 Modelling annual wood density variability**

335 The selection of the WD model resulted from the comparison of several models based
336 on independent variables such as ring width, cambial age and diameter. The models
337 offered very comparable results (Table 1) although model 2 had a greater Root Mean
338 Square Root (RMSE) and bias. Using cambial age or diameter as second independent
339 variable did not lead to significant differences in the fit according to the Likelihood
340 Ratio Test (LRT). Nevertheless, models differed in the ease of the convergence or on
341 the sensitivity to initial parameters provided. The exponent parameters a_2 and a_4 of the
342 independent variables (RW and X) being close to 0.5 in model 3, a simplification was
343 tested which enabled to reduce the number of parameters and considerably eased the
344 fitting, whereby both exponents were fixed to 0.5. This simplification did not lead to a
345 significant change in the AIC. The model retained was therefore the model 4 derived
346 from Eq. 3 with exponent parameters set to 0.5, and with the DBH as second
347 independent variable, which is also a variable easier to measure than the cambial age.

348

Olivier Bouriaud 8/7/15 15:27

Deleted: Although not really linear, the decrease of WD with ring width had a rate of -0.48 kg m⁻³ mm⁻¹, meaning that density is divided by two when ring width is doubling.

Olivier Bouriaud 8/7/15 15:50

Deleted: neither

Olivier Bouriaud 8/7/15 15:12

Deleted: more easy

355 Table 1.

356

357 **3.3 Modelling the annual volume increment**

358 The volume increment model was fit as a function of diameter and ring width, with
359 fixed and random tree-level effects, to a set of 22 trees. The intercept was kept free
360 after testing its significance using the LRT by comparing models with intercept held
361 constant or forced to 0. It appeared that a free intercept increases the likelihood, while
362 the estimated value of the intercept was very realistic. The use of a weight function
363 (constant plus power) was also amply confirmed by the LRT (L.ratio=1368,
364 $p < 0.0001$). Thus, the final model consisted in a function of diameter and ring width,
365 with fixed and random (tree level) parameters weighting (Table 2). The adequacy of
366 the model was confirmed by the standardized residuals plot (Fig. 2).

367

368 Figure 2.

369 Table 2.

370

371 **3.4 The compensation problem: WD buffers annual volume increment** 372 **variations**

373 Provided that there was an overall decrease in wood density with increasing ring
374 width, a compensation of ring width annual variability by wood density was also
375 probable. The ring width series showed peak years of growth (e.g. 1967, 1989) or
376 depressions (1976, 1983). In these years, the radial growth was much more affected
377 than the wood density, as suggested by the deviations relative to the mean value
378 calculated over the entire series length. The deviations peaked in 1967 at $+30 \pm 12\%$
379 (\pm standard error), which means a radial growth greater than average by 30%, while
380 the reduction of density was only $-5 \pm 2\%$. In 1976, the growth reduction was $-30 \pm 6\%$
381 but the density did not significantly increase: $+1 \pm 2\%$. The consequences for biomass
382 increment of neglecting the annual WD variations is further shown in Fig 3 where the
383 biomass increment was estimated for the trees used for WD measurements. The
384 annual volume increment was estimated by applying the model fitted (Eq. 4),

385 multiplied by either the annual WD values or by the mean WD for each tree and
386 radius. The deviation between the two estimates are expressed as a percentage of the
387 annual biomass increment using annual WD values. Although the deviations seemed
388 random (Fig. 3a), their ordination in time proved that they were not, and that they
389 exceeded 15% on average among all trees during extreme years (Fig. 3b).

390

391 Figure 3.

392

393 **3.5 Application to an independent data set**

394 The two models presented and fitted above were introduced in the Bayesian
395 framework, with the same structure exactly and on the same data, and further re-fitted
396 using the MCMC method. A comparison of the parameters estimated by both methods
397 is presented in table 2. Expectedly, the parameters were not exactly the same but very
398 close, and the correlation between the predictions was very high.

399 When applied on the independent application set, the estimated wood density varied
400 from 278 to 541 kg m⁻³, with a mean of 425 (±35) kg m⁻³ as a result of the variable
401 ring-width and diameter input values. The model reproduced large between-tree
402 differences for a given year, up to 225 kg m⁻³. Including random effects did not affect
403 the prediction mean (Fig. 4). The overall (pooling trees from all plots together)
404 average difference between the two predictions was only 0.1 kg m⁻³. The inclusion of
405 the random effects changed the predictions only very marginally but increased the
406 prediction interval five times: it jumped from ±20-40 kg m⁻³ to ±160 kg m⁻³.
407 Accounting for the residual variation (the epsilon term in Eq. 3) increased only
408 slightly the prediction interval: it added an extra ±10 kg m⁻³.

409 Comparable results were obtained with the volume increment model: the contribution
410 of the random effects and the inclusion of the residual variance inflated substantially
411 the prediction interval (Fig. 4). Nevertheless, the relative prediction interval were
412 substantially lower than that of the wood density: typically less than 40% of the
413 predicted value, against 60% for WD.

414

415 Figure 4.

416

417 3.6 Consequences of WD variations and error sources for the biomass 418 increment estimations

419 3.6.1 At tree level

420 The annual variations of the predicted biomass increment resulting from considering a
421 dynamic wood density were always smaller than predictions based on a constant
422 density (Fig. 5). The prediction uncertainty was considerably higher when accounting
423 for random effects on either the WD or the volume increment. The full error
424 propagation (sc4) had a relative prediction uncertainty up to 60% of the predicted
425 value on average, occasionally reaching or overcoming 100%. Constant density
426 predictions had logically the lowest uncertainties (less than 10%) since they include
427 only the error from the volume increment estimation. Wood density had the greatest
428 contribution to the prediction uncertainty, and mainly through the between-tree
429 variations. The parametric estimation (sc3) had a prediction interval four times lower
430 than the full error propagation prediction (sc4), showing an underestimation of the
431 error made by considering the uncertainty related to the regression coefficients only.

432

433 Figure 5.

434

435 3.6.2 At plot level

436 At plot level, which is the aggregation of the tree-level predictions and errors, the
437 prediction errors tended to compensate each other since the relative prediction
438 intervals of the annual biomass production were smaller than at tree-level (Fig. 6).
439 Thus the interval of biomass production estimates varied from ~7% (sc1: no random
440 effect, no residual error) to 10-30% (sc4: full error accounting) at stand level. It is
441 noticeable that the relative prediction interval at 95% was never greater than 40%
442 despite the combined errors of the two models (wood density and volume increment)
443 plus the errors related to the random tree-level variations.

444

Olivier Bouriaud 13/7/15 15:43

Deleted: The number of trees in the plot did not have a visible effect on the prediction errors and variations in the prediction interval were rather driven by the between-tree correlation (not shown). The variation between years in the prediction error was also very low (Fig. 6) despite contrasted ring widths. ... [1]

453
454
455
456
457
458
459
460

Figure 6.

The variation between years in the prediction error was also very low (Fig. 6) despite contrasted ring widths. The error of the predictions based on regression errors only (sc1 and sc3) did not vary with increasing number of trees in the plot (Fig. 6). In contrast, the predictions error decreased slightly with increasing number of trees for the scenarios that used a (tree-level) random-effect term (sc2 and sc4).

461 **4 Discussion**

462 **4.1 Overestimations of the variations in annual biomass increment under** 463 **constant density**

464 Wood density was found to decrease when ring width increased, in agreement with
465 previous studies on Norway spruce (e.g. Olesen, 1976; Lindström, 1996; Dutilleul et
466 al., 1998). Despite the seemingly high correlation between ring width and WD, the
467 decrease of WD was not enough to compensate the increase in ring width but
468 contributed to attenuate its effects. The order of magnitude of the WD variability was
469 not -and by far- as large as that of ring width. Hence, it is logical to find a moderate
470 compensation between radial growth and wood density variations even in extreme
471 years such as 1976: 15% at plot level. Nevertheless, when the focus is put on key
472 years, such as years of climatic extremes, the measurements of WD is necessary to
473 avoid a systematic underestimation of the biomass increment or carbon uptake.

474 Climate is indeed probably the most important driver of WD variations with
475 influences at both inter- and intra-annual time steps (e.g. Gindl et al. 2000, Bouriaud
476 et al. 2015). These results are consistent with those reported in Babst et al. (2014a)
477 showing that accounting for the variations in WD strongly improved the match
478 between the tree-ring based above-ground wood biomass increment estimations and
479 the seasonal CO₂ fluxes measured by eddy covariance.

480 A constant value of wood density, such as implicitly used in a biomass equations, can
481 generate systematic deviations because it has only few chances to be equal to the
482 mean density of the trees to which the model is applied. Even if using a site-specific
483 WD value, neglecting the radial increment of WD (i.e. the age-related trend) will also

Olivier Bouriaud 13/7/15 15:40

Deleted: -

Olivier Bouriaud 11/7/15 13:11

Deleted: in those years

Olivier Bouriaud 10/7/15 10:19

Deleted: 2013

487 lead to under-estimating the biomass increment. This source of error can
488 unfortunately not be compensated by a larger sampling since it affects all the trees
489 simultaneously. This has consequences not only for the annual productivity
490 estimations but also for periodical productivity assessments, such as those conducted
491 on permanent sample plots over a 5 or 10-year period.

492 Compensations of increased growth rate by a decrease in wood density was
493 documented for Norway spruce but over a long time scale (Bontemps et al., 2013).
494 The trends in radial growth and in WD reported for many species could lead to such
495 deviations between the actual WD and the modelled or implicit WD. In this context, a
496 local calibration would reduce such errors but cannot solve the problem of the
497 variations between years and between trees.

498 The anticorrelation between ring width and wood density seems to be a general
499 feature in Norway spruce according to the literature (e.g. Olesen, 1976; Lindström,
500 1996; Dutilleul et al., 1998) but the phenomenon is not limited to this species (Babst
501 et al., 2014). The attenuation therefore probably occurs at a large scale. The between-
502 tree variability in the relationship has also been reported in several studies and
503 probably is a widespread feature with potentially large consequences on the error of
504 annual biomass increment predictions, as demonstrated by this study. The fact that the
505 trees used to assess both the wood density variations and to model the volume
506 increment came from the same site as those used for the error estimations has ruled
507 out the issues of using locally inappropriate models. Additional errors should be
508 considered in practice when using models that may not be locally valid.

509 **4.2 Predictions uncertainty**

510 The inventory-based or tree-ring-based estimations of annual biomass production or
511 carbon uptake are often used for comparisons against other methods such as remote
512 sensing, vegetation models or eddy covariance (Beck et al., 2011; Bunn et al. 2013;
513 Babst et al., 2014a). To be conclusive, the benchmarking however supposes that
514 prediction errors are known or can be estimated. High prediction errors would
515 invalidate the biometric approaches but the errors are not always accounted for.
516 Analytical solutions are indeed not always available to estimate the errors of the
517 allometric models, and their estimation remains very complex or based on
518 assumptions. In the case of the biomass increment, the error results from the

519 combination of several models, and the estimation is even more challenging. The use
520 of the MCMC framework here avoids the cumbersome analytical approximations for
521 prediction variances (e.g. Wutzler et al., 2008).

522 The prediction interval at plot level was on average between 20 and 40% of the
523 predicted biomass increment value. The uncertainty related to the regression
524 parameters were about 10% only for both models. Reduced variance may be inherent
525 to the use of local trees and the Bayesian modelling (Zapata-Cuartas et al., 2012) but
526 these values are similar to those found by Nickless et al. (2011) for biomass
527 estimations following a parametric approach -as opposed to the MCMC method used
528 here. Unlike our results, this study did however not include the random tree-level
529 variations, which appeared to be quite an important source of uncertainty. Indeed,
530 accounting for random tree-level variations in the relation between wood density and
531 ring width increased the prediction interval of the tree-level biomass increment
532 drastically (i.e. decreased the prediction confidence), by a factor of 5. Further errors
533 related to the residual non-explained variance, were, in comparison, very small.
534 Consequently, the prediction interval of the biomass annual increment at plot level
535 increased twofold by accounting for the random-tree effects. Hence, the contribution
536 of WD to the prediction error of the biomass increment was much larger than that of
537 the volume increment model.

538 The tree-level prediction error (in percentage of the prediction value) was found to be
539 greater than those at plot level. Thus, the compensations occurred at plot level when
540 summing up trees predictions. We speculate that these compensations happen because
541 the variations are centred by construction around zero and have both negative and
542 positive values. This explains also why the mean prediction values were always
543 unaffected by accounting for random effects. Hence, neglecting random effects
544 affected more the prediction interval than the predictions themselves.

545

546 **4.3 Variations between trees**

547 The relation between wood density, ring width and cambial age were proven to
548 fluctuate between trees sampled within a same stand for many species: oak (Guilley et
549 al., 2004; Bergès et al., 2008), common beech (Bouriaud et al., 2004), Norway spruce
550 (Mäkinen et al., 2002; Jaakola et al., 2005; Franceschini et al., 2010). For a given

551 radial growth rate, the trees are building more or less biomass and so storing more or
552 less carbon, according to the density of the wood.

553 This fluctuation is considered random because it cannot be attributed to a measurable
554 factor. Random tree-level variations were nevertheless reported as a major source of
555 wood density variations in a population (Zhang et al., 1994; Guilley et al., 2004;
556 Bouriaud et al., 2004; Jaakola et al., 2005). It is often hypothesized to be related to the
557 genetics, although not proven. Provenience studies brought some insight on it (Hysten,
558 1999; Rozenberg et al., 2004), but much of the determinism remains unknown. Other
559 factors, such as crown development (Lindström, 1996), could also be invoked to
560 explain this variation source in wood density.

561 The changes in silvicultural practices, whereby the focus is put on targeted
562 individuals, further stress the importance of errors in tree-level estimations of biomass
563 and biomass increments. The tree-level variations were the largest error source and
564 showed that the inter-tree variations can be seen as a limitation to the tree-level
565 biomass prediction. Despite the many evidences of tree-level random effects, this
566 variation source was largely ignored. Our study proved that the between-tree
567 variations in the relation between ring width and wood density -although within the
568 same species- contributed the most to the uncertainty in the biomass increment
569 predictions. The variations are hypothesized to follow a normal distribution
570 (Lindström and Bates, 1990). Thus, at plot level, a compensation is likely to occur.
571 But this situation may not be true for all samplings, and certain designs could generate
572 additional biases in the biomass production estimations. In this study, all the trees in a
573 plot were sampled. Other samplings, for instance the selection of the biggest trees in a
574 plot as classically done in dendrochronology, could lead to serious deviations as it
575 could involve sampling faster-growing trees. Apart from the bias in productivity
576 caused by a sampling focusing on faster-growing trees (Nehrbass-Ahles et al., 2014),
577 the productivity at stand level would probably generate an over-estimation related to a
578 decreased wood density as trees producing larger rings would be sampled. Another
579 issue in using the tree-ring parameters (width and density) to produce annual
580 productivity estimations is the presence of autocorrelation or carry-over effects in the
581 series, which are reflected in the derived productivity estimations but are generally
582 not observed in the carbon fluxes measured or modeled (Babst et al. 2014a, b,
583 Ramming et al. 2015).

585 4.4 Modelling wood density for biomass increment

586 | ~~Apart from the climate,~~ the two foremost used variables used to model annual WD
587 variations are ring width and ring (cambial) age. The relation between WD and radial
588 growth was strong in our study and probably dominant in Norway spruce but may not
589 be so for other species. In beech, for example, the relation between ring width and
590 WD was shown to be weak (Bouriaud et al., 2004) and there was no clear trend in
591 WD related to the age neither. Several studies reported a lack of significant
592 correlations between ring width and WD for Norway spruce (e.g. Dutilleul et al.,
593 1998). The relative stability in annual WD values is not calling for a correction of the
594 biomass increment in such situation. It is probable that variations in WD would affect
595 the estimation of biomass increment in species for which a relationship with ring
596 width was already observed such oaks (Zhang et al., 1993; Bergès et al., 2008) or
597 larch (Karlman et al., 2005). The contribution to the error in the prediction of biomass
598 production is however likely to be important.

599 Conversely to ring width, ring age was found to be only slightly influent on the annual
600 wood density in Norway spruce. Ring age is often considered in density models for
601 representing the age trend or for the variations observed near the pith –the juvenile
602 versus mature wood transition (e.g. Franceschini et al., 2010). WD in Norway spruce
603 has been shown to present an age-dependent trend from pith to bark (Dutilleul et al.,
604 1998; Hysten, 1999; Mäkinen et al., 2002), apart from the juvenile wood effect. In our
605 study, the juvenile effect was not included for simplicity (series were pruned to
606 | exclude the first 3 years) but also because rings near pith anyway ~~are~~ often ~~missing~~
607 when working with increment cores. Part of the age effect can be absorbed by the
608 irregular ring width variations exhibited by trees growing in stands where thinnings
609 induce successive episodes of growth surge.

610 Wood density should not be mistaken for stem specific gravity (Williamson et al.,
611 2010). Bark has a different mass to volume ratio than wood. The contribution of bark
612 to the annual increment is however negligible. The approximation made consist in
613 stating that the variations in specific gravity are proportional to that of wood density.
614 Variations in ring width and WD at upper stem positions were however documented
615 | for different species (Bouriaud et al., 2005; Repola, 2006; Van der Maaten-

Olivier Bouriaud 11/7/15 11:58

Deleted: T

617 [Theunissen](#) and Bouriaud, 2012). These variations were mostly in the sense of a lesser
618 reduction in growth of upper stem parts during years of limited growth. Altogether
619 with the WD density effect, these effects show that the reaction of trees to
620 unfavourable climate conditions are exacerbated or over-estimated by the breast-
621 height radial growth.

622

623 **5 Conclusion**

624 Annual variations in wood density were proved to compensate partially (up to 15%)
625 the variations in radial growth. Ignoring the relation between ring width and wood
626 density would result in an underestimation of the biomass production in bad years.
627 The use of allometric equations generated estimations with large prediction intervals
628 at tree level, up to 60%, but the prediction errors at plot level compensated [each other](#).
629 Most of the error in the prediction of a tree's annual biomass increment comes from
630 the great between tree variability in wood density. Plot-level errors were found to
631 range between 10 and 20% only. This study validates the approach based on historical
632 diameter records for estimating tree annual biomass increment and stand annual
633 biomass production, but a local calibration of the allometric models reduces
634 considerably the prediction errors.

635

636 **6 Acknowledgements**

637 This work was supported by a grant of the Romanian National Authority for Scientific
638 Research, CNCS-UEFISCDI, project number PN-II-ID-PCE-2011-3-0781. CW is
639 thankful to Sebastian Weist and Ulrich Pruschitzki for help in the field and Anja Kahl
640 for dendrochronological analysis. CW acknowledges the support of the Max-Planck
641 Society. AVK acknowledges EU COST Action FP1106 STReESS. [Ernst-Detlef](#)
642 Schulze and Reiner Zimmermann established the Wetzstein site.

643

644 **7 References**

- 645 Anthoni, P. M., Knohl, A., Rebmann, C., Freibauer, A., Mund, M., Ziegler, W., Kolle,
646 O., and Schulze, E.D.: Forest and agricultural land use dependent CO₂ exchange in
647 Thuringia, Germany. *Glob. Change Biol.*, 10(12), 2005-2019, 2004.
- 648 Babst, F., Poulter, B., Trouet, V., Tan, K., Neuwirth, B., Wilson, R., Carrer, M.,
649 Grabner, M., Tegel, W., Levanic, T., Panayotov, M., Urbinati, M., Bouriaud, O.,
650 Ciais, P., and Frank, D.: Site- and species-specific responses of forest growth to
651 climate across the European continent. *Glob. Ecol. Biogeogr.*, 22(6), 706-717.
652 doi: 10.1111/geb.12023, 2013.
- 653 Babst, F., Bouriaud, O., Papale, D., Gielen, B., Janssens, I.A., Nikinmaa, E., Ibrom,
654 A., Wu, K., Bernhofer, C., Köstner, B., Grünwald, T., and Frank, D.: Above-ground
655 woody carbon sequestration measured from tree rings is coherent with net ecosystem
656 productivity at five eddy-covariance sites. *New Phytol.*, 201, 1289-1303.
657 DOI: 10.1111/nph.12589, 2014a.
- 658 [Babst, F., Alexander, M. R., Szejner, P., Bouriaud, O., Klesse, S., Roden, J., Ciais, P.,](#)
659 [Poulter, B., Frank, D., Moore, J. P. and Trouet, V.: A tree-ring perspective on the](#)
660 [terrestrial carbon cycle. *Oecologia*, 176\(2\), 307-322, 2014b.](#)
- 661 Barford, C.C., Wofsy, S.C., Goulden, M.L., Munger, J.W., Pyle, E.H., Urbanski, S.
662 P., Hutyra L., Saleska S.R., Fitzjarrald D., and Moore, K.: Factors controlling long-
663 and short-term sequestration of atmospheric CO₂ in a mid-latitude forest. *Science*,
664 294(5547), 1688-1691, 2001.
- 665 Beck, P.S.A., Juday, G.P., Alix, C., Barber, V.A., Winslow, S.E., Sousa, E.E., Heiser,
666 P., Herriges, J.D., and Goetz, S.J.: Changes in forest productivity across Alaska
667 consistent with biome shift. *Ecol. Lett.*, 14, 373–379, 2011.
- 668 Beer, C., Reichstein, M., Tomelleri, E., Ciais, P., Jung, M., Carvalhais, N.,
669 Rödenbeck, C., Arain, M. A., Baldocchi, D., Bonan, G. B., Bondeau, A., Cescatti, A.,
670 Lasslop, G., Lindroth, A., Lomas, M., Luyssaert, S., Margolis, H., Oleson, K. W.,
671 Rouspard, O., Veenendaal, E., Viovy, N., Williams, C., Woodward, F. I., and Papale,
672 D.: Terrestrial gross carbon dioxide uptake: global distribution and covariation with
673 climate, *Science*, 329, 834–838, 2010.

674 Bergès, L., Nepveu, G., and Franc, A.: Effects of ecological factors on radial growth
675 and wood density components of sessile oak (*Quercus petraea* Liebl.) in Northern
676 France. *Forest Ecol. Manage.*, 255(3), 567-579, 2008.

677 Bergqvist, G.: Wood density traits in Norway spruce understorey: effects of growth
678 rate and birch shelterwood density. *Ann. Sci. For.*, 55(7), 809-821, 1998.

679 Bontemps, J.D., Gelhaye, P., Nepveu, G., and Hervé, J.C.: When tree rings behave
680 like foam: moderate historical decrease in the mean ring density of common beech
681 paralleling a strong historical growth increase. *Ann. Sci. For.*, 70(4), 1-15, 2013.

682 Bouriaud, O., Breda, N., Le Moguedec, G., and Nepveu, G.: Modelling variability of
683 wood density in beech as affected by ring age, radial growth and climate. *Trees-*
684 *Struct. Func.*, 18, 264-276, 2004.

685 Bouriaud, O., Leban, J.M., Bert, D., and Deleuze, C.: Intra-annual variations in
686 climate influence growth and wood density of Norway spruce. *Tree Physiol.*, 25(6),
687 651-660, 2005.

688 Bunn, A.G., Hughes, M.K., Kirilyanov, A.V., Losleben, M., Shishov, V.V., Berner,
689 L.T., Oltchev, A., and Vaganov, E.A. 2013. Comparing forest measurements from
690 tree rings and a space-based index of vegetation activity in Siberia. *Environ. Res.*
691 *Lett.* 8, 035034, 2013. doi:10.1088/1748-9326/8/3/035034.

692 Ciais, P., Reichstein, M., Viovy, N., Granier, A., Oée, J., Allard, V., Aubinet, M.,
693 Buchmann, N., Bernhofer, C., and Carrara, A.: Europe-wide reduction in primary
694 productivity caused by the heat and drought in 2003: *Nature*, 437, 529–533, 2005.

695 Ciais, P., Schelhaas, M.J., Zaehle, S., Piao, S.L., Cescatti, A., Liski, J., Luysaert, S.,
696 Le-Maire, G., Schulze, E.-D., Bouriaud, O., Freibauer, A., Valentini R., and Nabuurs,
697 G.J.: Carbon accumulation in European forests. *Nat. Geoscience*, 1, 425–429,
698 doi:10.1038/ngeo233, 2008.

699 Curtis, P., Hanson, P., Bolstad, P., Barford, C., Randolph, J., Schmid, H., and Wilson,
700 K.: Biometric and eddy-covariance based estimates of annual carbon storage in five
701 eastern North American deciduous forests. *Agr. Forest Meteorol.*, 113, 3-19, 2002.

702 Dutilleul, P., Herman, M., and Avella-Shaw, T.: Growth rate effects on correlations
703 among ring width, wood density, and mean tracheid length in Norway spruce (*Picea*
704 *abies*). *Can. J. Forest Res.*, 28(1), 56-68, 1998.

- 705 Evans, R.: Rapid Measurement of the Transverse Dimensions of Tracheids in Radial
706 Wood Sections from *Pinus Radiata*. *Holzforschung*, 48(2), 168-172, 1994.
- 707 Franceschini, T., Bontemps, J.D., Gelhaye, P., Rittie, D., Herve, J.C., Gegout, J.C.,
708 and Leban, J.M.: Decreasing trend and fluctuations in the mean ring density of
709 Norway spruce through the twentieth century. *Ann. For. Sci.*, 67(8), 2010.
- 710 Franceschini, T., Longuetaud, F., Bontemps, J.D., Bouriaud, O., Caritey, B.D., and
711 Leban, J.M.: Effect of ring width, cambial age, and climatic variables on the within-
712 ring wood density profile of Norway spruce *Picea abies* (L.) Karst. *Trees-Struct.*
713 *Func.*, 27(4), 913-925, 2013.
- 714 [Gindl, W., Grabner, M., Wimmer, R.: The influence of temperature on latewood](#)
715 [lignin content in treeline Norway spruce compared with maximum density and ring](#)
716 [width. *Trees-Struct. Func.*, 14, 409-414, 2000.](#)
- 717 Gough, C., Vogel, C., Schmid, H., and Curtis, P.: Controls on annual forest carbon
718 storage: Lessons from the past and predictions for the future. *Bioscience*, 58: 609-622,
719 2008.
- 720 Guilley, E., Hervé, J.C., and Nepveu, G.: The influence of site quality, silviculture
721 and region on wood density mixed model in *Quercus petraea* Liebl. *Forest Ecol.*
722 *Manage.*, 189(1), 111-121, 2004.
- 723 Hysten, G.: Age trends in genetic parameters of wood density in young Norway
724 spruce. *Can. J. Forest Res.*, 29(1), 135-143, 1999.
- 725 Ikonen, V. P., Peltola, H., Wilhelmsson, L., Kilpeläinen, A., Väisänen, H., Nuutinen,
726 T., and Kellomäki, S.: Modelling the distribution of wood properties along the stems
727 of Scots pine (*Pinus sylvestris* L.) and Norway spruce (*Picea abies* (L.) Karst.) as
728 affected by silvicultural management. *Forest Ecol. Manage.*, 256(6), 1356-1371,
729 2008.
- 730 Ilvesniemi, H., Levula, J., Ojansuu, R., Kolari, P., Kulmala, L., Pumpanen, J.,
731 Launiainen, S., Vesala, T., and Nikinmaa, E.: Long-term measurements of the carbon
732 balance of a boreal Scots pine dominated forest ecosystem. *Boreal Environmental*
733 *Research*, 14, 731-753, 2009.
- 734 Jaakkola, T., Mäkinen, H., and Saranpää, P. Wood density in Norway spruce: changes
735 with thinning intensity and tree age. *Can. J. Forest Res.*, 35(7), 1767-1778, 2005.

736 Jyske, T., Makinen, H., and Saranpaa, P.: Wood density within Norway spruce stems.
737 *Silva Fenn.*, 42(3), 439-455, 2008.

738 Karlman, L., Mörling, T., and Martinsson, O.: Wood density, annual ring width and
739 latewood content in larch and Scots pine. *Eurasian J. Forest Res.*, 8(2), 91-96, 2005.

740 Lindström, H.: Basic density of Norway spruce. Part II. Predicted by stem taper, mean
741 growth ring width, and factors related to crown development. *Wood Fiber Sci.*, 28(2),
742 240-251, 1996.

743 Lindström, M.J., Bates, D.M.: Nonlinear mixed effects models for repeated measures
744 data. *Biometrics*, 673-687, 1990.

745 Lundgren, C.: Microfibril angle and density patterns of fertilized and irrigated
746 Norway spruce. *Silva Fenn.*, 38(1), 107-117, 2004.

747 Mäkinen, H., Saranpää, P., and Linder, S.: Wood-density variation of Norway spruce
748 in relation to nutrient optimization and fibre dimensions. *Can. J. Forest Res.*, 32(2),
749 185-194, 2002.

750 Molto, Q., Rossi, V., and Blanc, L.: Error propagation in biomass estimation in
751 tropical forests. *Methods Ecol. Evol.*, 4, 175-183, doi:10.1111/j.2041-
752 210x.2012.00266.x, 2012.

753 Nehrbass-Ahles, C., Babst, F., Klesse, S., Nötzli, M., Bouriaud, O., Neukom, R.,
754 Dobbertin, M., and Frank, D.: The influence of sampling design on tree-ring based
755 quantification of forest growth. *Glob. Change Biol.*, 20(9), 2867-2885, 2014.

756 Nickless, A., Scholes, R.J., and Archibald, S.: Calculating the variance and prediction
757 intervals for estimates obtained from allometric relationships. *S. Afr. J. Sci.*
758 2011;107(5/6), Art. #356, doi:10.4102/sajs.v107i5/6.356, 2011.

759 Ohtsuka T, Mo W, Satomura T, Inatomi M, and Koizumi H.: Biometric based carbon
760 flux measurements and net ecosystem production (NEP) in a temperate deciduous
761 broad-leaved forest beneath a flux tower. *Ecosystems*, 10, 324-334, 2007.

762 Pinheiro, J., Bates, D., DebRoy, S., and Sarkar, D.: R Development Core Team (2011)
763 nlme: linear and nonlinear mixed effects models. R package version 3.1-98. R
764 Foundation for Statistical Computing, Vienna, 2011.

765 [Ramming, A., Wiedermann, M., Donges, J.F., Babst, F., von Bloh, W., Frank, D.,](#)
766 [Thonicke, K. and Mahecha, M.D.: Coincidences of climate extremes and anomalous](#)
767 [vegetation responses: comparing tree ring patterns to simulated productivity.](#)
768 [Biogeosciences, 12, 373-385, 2015.](#)

769 Repola, J.: Models for vertical wood density of Scots pine, Norway spruce and birch
770 stems, and their application to determine average wood density. *Silva Fenn.*, 40(4),
771 673-685, 2006.

772 Rey, A.N.A., and Jarvis, P.: Modelling the effect of temperature on carbon
773 mineralization rates across a network of European forest sites (FORCAST). *Glob.*
774 *Change Biol.*, 12(10), 1894-1908, 2006.

775 Reichstein, M., Ciais, P., Papale, D., Valentini, R., Running, S., Viovy, N., Cramer,
776 W., Granier, A., Ogee, J., Allard, V., Aubinet, M., Bernhofer, C., Buchmann, N.,
777 Carrara, A., Grünwald, T., Heimann, M., Heinesch, B., Knohl, A., Kutsch, W.,
778 Loustau, D., Manca, G., Matteucci, G., Miglietta, F., Ourcival, J. M., Pilegaard, K.,
779 Pumpanen, J., Rambal, S., Schaphoff, S., Seufert, G., Soussana, J. F., Sanz, M. J.,

780 Rey, A.N.A., and Jarvis, P.: Modelling the effect of temperature on carbon
781 mineralization rates across a network of European forest sites (FORCAST). *Glob.*
782 *Change Biol.*, 12(10), 1894-1908, 2006.

783 Richardson, A. D., Black, T. A., Ciais, P., Delbart, N., Friedl, M. A., Gobron, N.,
784 Hollinger, D. Y., Kutsch, W. L., Longdoz, B., and Luysaert, S.: Influence of spring
785 and autumn phenological transitions on forest ecosystem productivity, *Philos. T. R.*
786 *Soc. B*, 365, 3227–3246, 2010.

787 Rocha A, Goulden M, Dunn A, and Wofsy S.: On linking interannual tree ring
788 variability with observations of whole-forest CO₂ flux. *Glob. Change Biol.*, 12, 1378-
789 1389, 2006.

790 Rozenberg, P., Schüte, G., Ivkovich, M., Bastien, C., and Bastien, J.C.: Clonal
791 variation of indirect cambium reaction to within-growing season temperature changes
792 in Douglas-fir. *Forestry*, 77, 257–268, 2004.

793 Spiegelhalter, D.J., Thomas, A., Best, N., and Lunn, D.: WinBugs 1.4 [computer
794 program]. Cambridge, UK: MRC Biostatistics Unit, Cambridge University, 2003.

795 Schweingruber, F.H.: *Tree rings and environment: dendroecology*. Paul Haupt AG
796 Bern, 1996.

797 van der Maaten-Theunissen, M., and Bouriaud, O.: Climate–growth relationships at
798 different stem heights in silver fir and Norway spruce. *Can. J. Forest Res.*, 42(5), 958-
799 969, 2012.

800 Vesala, T., and Zhao, M.: Reduction of ecosystem productivity and respiration during
801 the European summer 2003 climate anomaly: a joint flux tower, remote sensing and
802 modelling analysis, *Glob. Change Biol.*, 13, 634–651, 2007.

803 Vilà, M., Carrillo-Gavilán A., Vayreda J., Bugmann H., Fridman J., Grodzki W.,
804 Haase J., Kunstler G., Schelhaas M.J., and Trasobares A.. "Disentangling Biodiversity
805 and Climatic Determinants of Wood Production." *PloS One*, 8(2), e53530, 2013.

806 Wilhelmsson, L., Arlinger, J., Spångberg, K., Lundqvist, S.O., Grahn, T., Hedenberg,
807 Ö., and Olsson, L.: Models for predicting wood properties in stems of *Picea abies* and
808 *Pinus sylvestris* in Sweden. *Scand. J. Forest Res.*, 17(4), 330-350, 2002.

809 Williamson, G.B., and Wiemann, M.C.: Measuring wood specific gravity... correctly.
810 *Am. J. Bot.*, 97(3), 519-524, 2010.

811 Wimmer, R., and Downes, G.M.: Temporal variation of the ring width-wood density
812 relationship in Norway spruce grown under two levels of anthropogenic disturbance.
813 *IAWA*, 24(1): 53-61, 2003.

814 Wirth, C., Schumacher, J., and Schulze, E.D.: Generic biomass functions for Norway
815 spruce in Central Europe—a meta-analysis approach toward prediction and
816 uncertainty estimation. *Tree Physiol.*, 24(2), 121-139, 2004.

817 Wu, X., Mahecha, M.D., Reichstein, M., Ciais, P., Wattenbach, M., Babst, F., Frank,
818 D., and Zang, C.: Climate-mediated spatiotemporal variability in the terrestrial
819 productivity across Europe. *Biogeosciences Discuss.*, 10, 17511–17547, 2013.

820 Wutzler, T., Wirth, C., and Schumacher, J.: Generic biomass functions for Common
821 beech (*Fagus sylvatica*) in Central Europe: predictions and components of
822 uncertainty. *Can. J. Forest Res.*, 38(6), 1661-1675, 2008.

823 Zapata-Cuartas, M., Sierra, C.A., and Alleman, L.: Probability distribution of
824 allometric coefficients and Bayesian estimation of aboveground tree biomass. *Forest
825 Ecol. Manage.*, 277, 173-179, 2012.

826 Zhang, S.Y., Owoundi, R.E., Nepveu, G., Mothe, F., and Dhôte, J.F.: Modelling wood
827 density in European oak (*Quercus petraea* and *Quercus robur*) and simulating the
828 silvicultural influence. Can. J. Forest Res., 23(12), 2587-2593, 1993.

829 Zhang, S.Y., Nepveu, G., and Owoundi, R.E.: Intratree and intertree variation in
830 selected wood quality characteristics of European oak (*Quercus petraea* and *Quercus*
831 *robur*). Can. J. Forest Res., 24(9), 1818-1823, 1994.

832

833 **Tables and figure captions**

834 Table 1. Fit statistics and parameters for the wood density models.

835 Table 2. Comparison of the fixed parameters estimated for the wood density and the
836 volume models, obtained by maximum likelihood and MCMC. Standard deviations
837 are provided in brackets.

838

839 Figure 1. Relation between annual wood density and cambial age (left) or ring width
840 (right) at tree level. Two trees with very distinct average wood density were
841 highlighted (dark gray/black colors).

842

843 Figure 2. Observed and fitted annual volume increment model and standardized
844 residuals of the volume increment model fit.

845

846 Figure 3. Left, Comparison of biomass increment estimations for Norway spruce trees
847 growing in Wetzstein, based on constant density hypothesis vs actual wood density
848 measurements; Right, time-course of the average ratio of biomass increment
849 estimations (actual over constant density) and time-course of the detrended mean ring
850 width (spline smoothing, for illustration purposes).

851 The $\pm 2sd$ interval for the average biomass ratio is displayed as a gray band.

852

853 Figure 4. Left, variations of the MCMC annual predictions and prediction intervals
854 (95%) of wood density and volume increment for one given tree randomly chosen
855 while accounting for different error sources: regression only/regression and random
856 effects/regression, random effects and residual variance; Right, distribution density of
857 the relative prediction interval (expressed in percentage of the prediction) for all trees
858 used for the simulation, according to the error sources included.

859

860 Figure 5. Annual biomass increment (posterior MCMC distribution) for one given tree
861 chosen as representative with its associated prediction error for scenario 1 and 2 (a) or

Olivier Bouriaud 4/8/15 10:46

Deleted:

863 scenario 3 and 4 (b); c) distribution density of relative prediction interval (expressed
864 in percent of the prediction) for all trees used for the simulation, according to the
865 scenario. Scenario 1 is based on constant WD and no random or residual error from
866 the volume increment model, Scenario 2 is based on constant WD and random error
867 in the volume increment model, Scenario 3 is based on modelled WD but without
868 random and residual error accounting, Scenario 4 is based on modelled WD and
869 volume increment with a full error accounting (see section 2.3 for more details).

870

871 | Figure 6. Plot-level annual relative prediction intervals of the biomass increment as a
872 | function of the number of trees sampled in the plot for the 4 scenarios (a). Distribution
873 | density of the relative prediction interval of the biomass increment at plot level, all
874 | plots pooled, (b).

875
876

- Olivier Bouriaud 13/7/15 15:56
Deleted: Comparison of plot-level annual biomass increments
- Olivier Bouriaud 13/7/15 15:58
Deleted: (a) and prediction intervals (b) for
- Olivier Bouriaud 13/7/15 15:57
Deleted: c

881

Table 1

882

Eq.	Model	Fixed effect	df	AIC	RMSE	Bias
					kg.m ⁻³	kg.m ⁻³
1	WD = $a_0 + a_1 \cdot RW + a_2 \cdot RW^2 + a_3 / X^{0.5}$	RW, CBA	12	12549	44.62	0.135
		RW, DBH	12	12567	44.90	0.135
2	WD = $a_0 + a_1 / (1 + RW) + a_2 / X^{0.5}$	RW, CBA	11	12770	60.24	0.874
		RW, DBH	11	12802	64.70	0.674
3	WD = $a_0 + a_1 \cdot RW^{a_2} + a_3 / X^{a_4}$	RW, CBA	12	12554	44.90	0.018
		RW, DBH	12	12569	45.15	-0.046
4	WD = $a_0 + a_1 RW^{0.5} + a_2 / X^{0.5}$	RW, CBA	11	12552	44.92	-0.019
		RW, DBH	11	12567	45.20	-0.073

883

884

885

886

887

888

889

WD: (annual) wood density, RW: (annual) ring width, X: either cambial age (CBA) or diameter (DBH).

Models 1 to 3 correspond to equations 1-3 presented in the section 2.2.1, and model 4 corresponds to equation 3 with parameter a_2 and a_4 set to 0.5.

They were 1201 observations, 10 groups.

Olivier Bouriaud 13/7/15 16:03

Deleted: ^{0.5}

891

Table 2

892

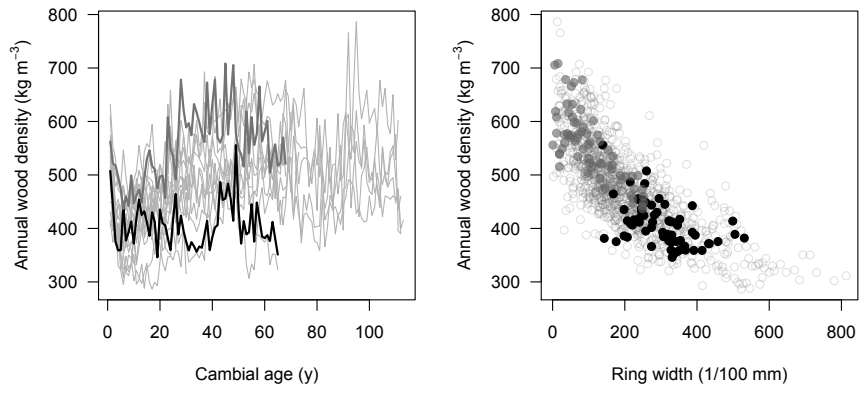
Model	Parameters	Likelihood fit	MCMC fit
WD = $a_0 + a_1 RW^{0.5} + a_2 / DBH^{0.5} + e$	a_0	594.33 (16.11)	555.10 (20.04)
	a_1	-10.09 (0.43)	-9.23 (0.70)
	a_2	13.93 (41.21)	17.13 (29.00)
	e	2054	2083 (93)
$\Delta V = b_0 + b_1 DBH^{b_2} RW^{b_3} + e$	b_0	0.284 (0.041)	0.047 (0.005)
	b_1	0.161 (0.012)	0.009 (0.001)
	b_2	1.820 (0.034)	1.733 (0.011)
	b_3	0.645 (0.019)	0.649 (0.019)
	$e = b_4 + DBH^{b_5}$	9.316e-03	0.283 (0.136)
	b_4	15.505	-0.093 (0.009)
	b_5	1.871	0.225 (0.005)

893 WD: (annual) wood density, RW: (annual) ring width, DBH: (annual) breast-height diameter, e:
894 residual error.

895

896

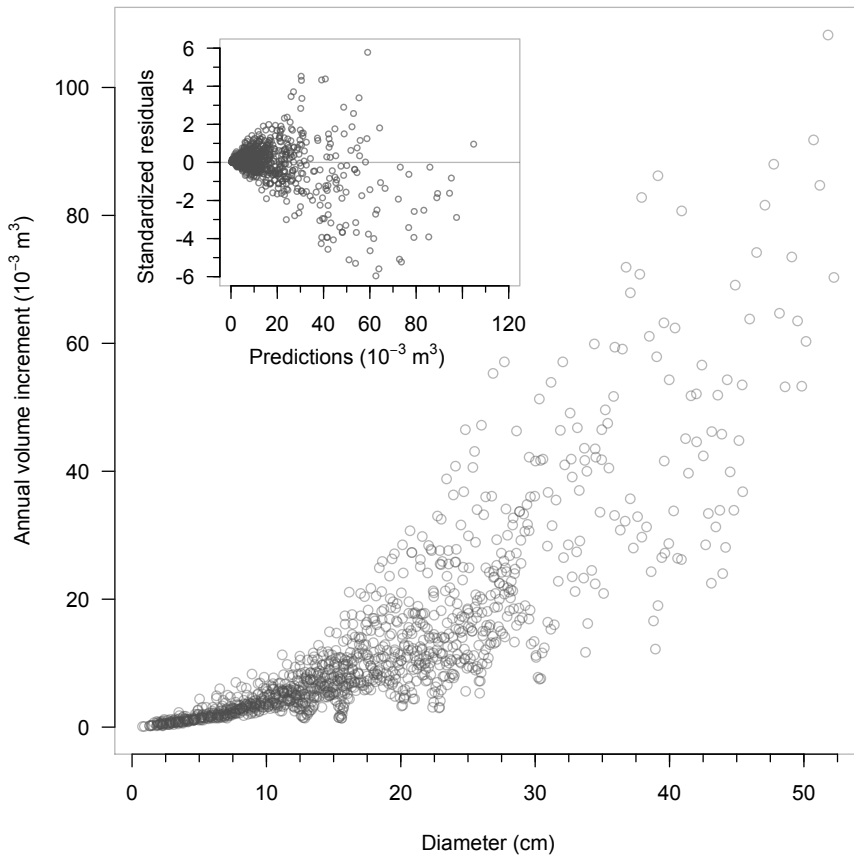
Figure 1



897

898

Figure 2



900

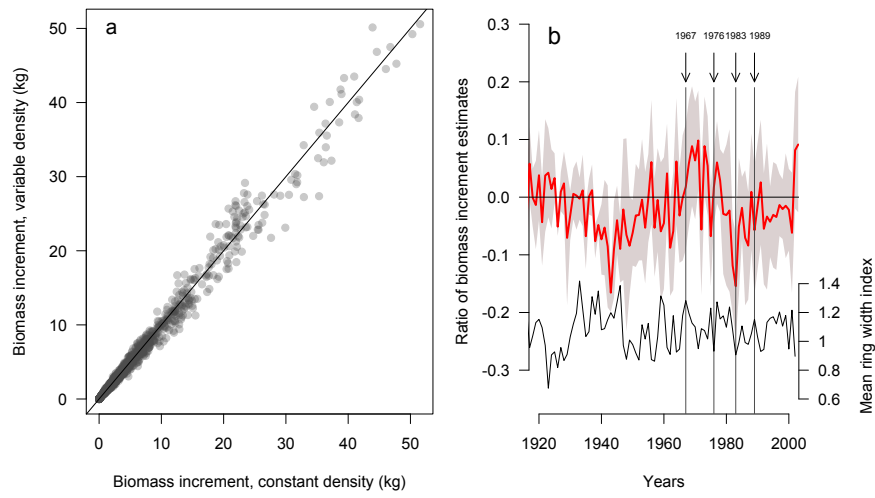
901

902

903

Figure 3

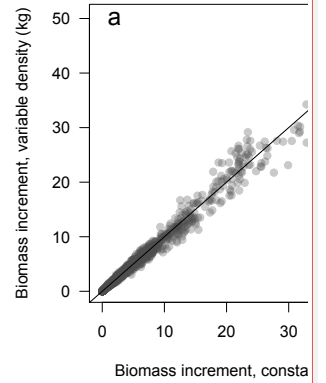
904



905

906

Olivier Bouriaud 13/7/15 15:46



Deleted:

Figure 4

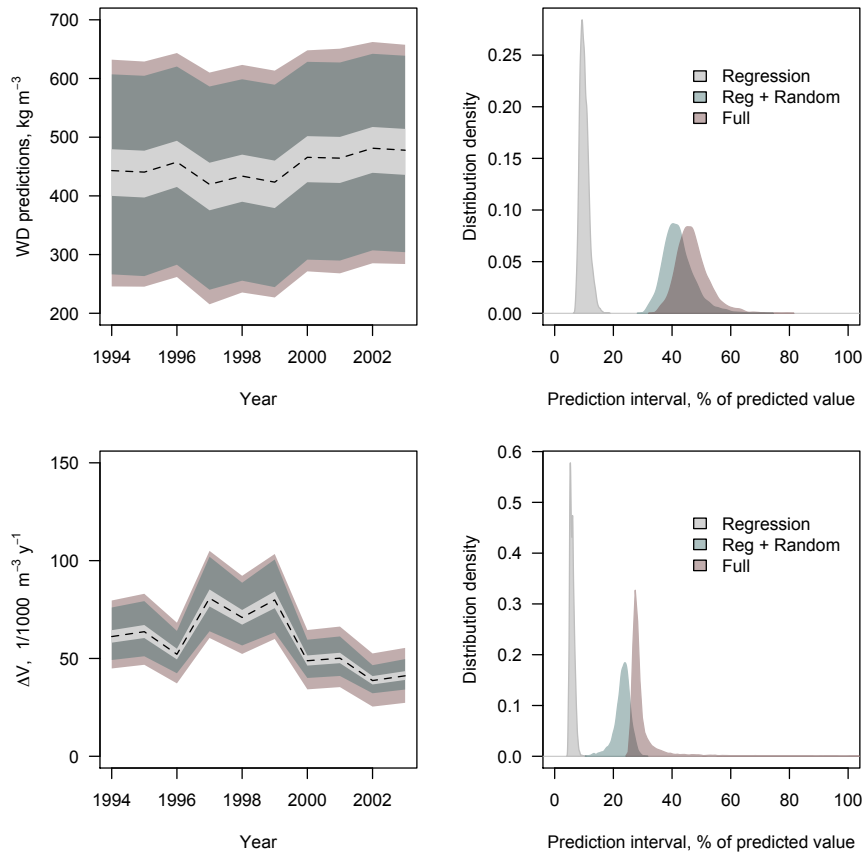
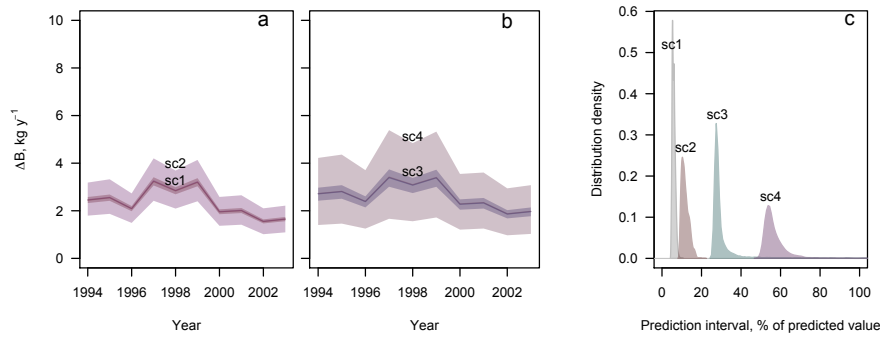


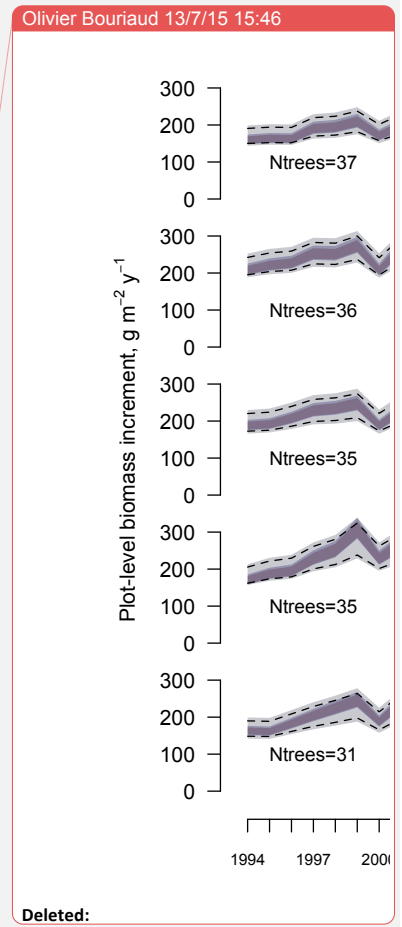
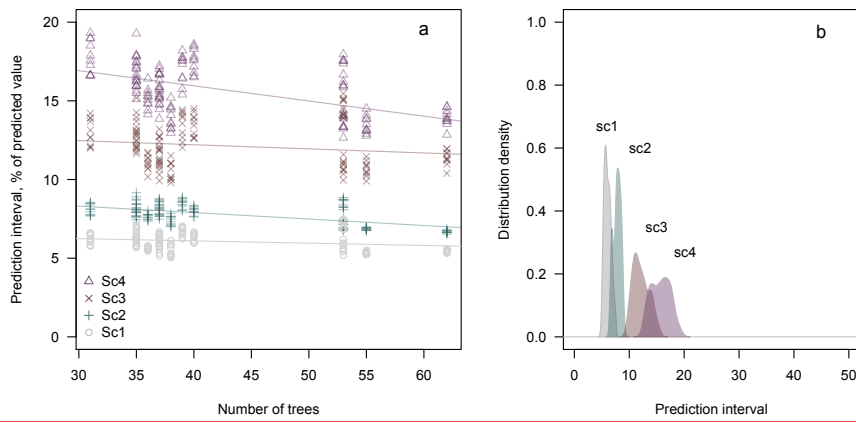
Figure 5



912

913

Figure 6



Deleted: